Anisotropic flux dynamics in single-crystalline and melt-textured $YBa_2Cu_3O_{7-\delta}$

Vjacheslav F. Solovjov
Institute for Metal Physics, 36 Vernadsky Boulevard, 252142 Kiev, Ukraine

Vladimir M. Pan
Institute for Metal Physics, 36 Vernadsky Boulevard, 252142 Kiev, Ukraine
and Institute for Metal Physics, University of Goettingen, Hospitalstraße 3-7, 37073 Goettingen, Germany

Herbert C. Freyhardt
Institute for Metal Physics, University of Goettingen, Hospitalstraße 3-7, 37073 Goettingen, Germany
(Received 26 May 1994)

Direct transport measurements of the angular dependencies of the critical current density for single-crystalline and melt-textured $YBa_2Cu_3O_{7-\delta}$ have been carried out in the temperature range between 77 K and T_c and applied magnetic fields up to 2.0 T. In contrast to the melt-textured samples, the $J_c(\theta)$ dependencies for the twinned single crystals reveal a minimum in the $\mathbf{H}\|c$ configuration ($\theta=0$). The nonmonotonic $J_c(H)$ behavior (fishtail effect) appeared to be much more pronounced in tilted magnetic fields. The fishtail as well as the $J_c(\theta)$ minimum at $\mathbf{H}\|c$ were shown to depend strongly on the E_c criterion for J_c definition. An E_c increase by two orders of magnitude suppresses the fishtail and transforms the $J_c(\theta)$ minimum to a maximum. Two alternative approaches for the flux dynamics were used: (i) thermally activated-vortex-hopping theories and (ii) the classical mean-field approximation (MFA). The MFA analyses of the I-V curves for the different θ, H, and T were much more consistent and informative. In the case of the flux-line lattice (FLL) moving in the pinning potential there should exist a region (defined by the level of dissipation) between creep-controlled FLL motion and Bardeen-Stephen flow. In this region a key role is played by not only the depth of the pinning wells but also the features of the pinning potential, elastic, and viscous properties of the FLL. A scaling behavior predicted by the MFA analysis was observed for the low-field I-V curves. A breakdown of scaling was detected when the "fishtail effect" arose. The fishtail effect is shown to have a dynamic nature. It is controlled by vortex interaction with random pointlike disorder and influenced strongly by the FLL relaxation if the relaxation and pinning times are comparable. The twins are supposed to promote a correlated disorder and inhibit the three-dimensional pointlike random disorder as a dominant state for the pinning of the FLL. This is a reason for the J_c minimum at $\mathbf{H}\|\mathbf{c}$, observed at the low level of dissipation.

I. INTRODUCTION

The critical current density J_c of high-T_c superconductors (HTSC's) has been found to be anisotropic, with the maximum J_c occurring when an external magnetic field is applied parallel to the *ab* plane. Such a strong sensitivity of J_c to the magnetic-field orientation has been observed in thin films as well as in melt-textured (MT) $YBa_2Cu_3O_{7-\delta}$ (YBCO) samples.[1,2] Since the J_c maximum has usually been accounted for by so-called intrinsic pinning,[3] most researchers were convinced that in YBCO single crystals (SC's) the situation in general should be the same but more pronounced. Indeed, the intrinsic pinning caused by superconducting-order-parameter modulation along the *c*-axis direction is assumed to be greater in SC's as a consequence of their greater structural perfection. Unexpectedly, the real situation appears to be quite different for YBCO SC's, at least for low and intermediate magnetic fields (up to 1.5–2.0 T) at high enough temperatures. Moreover, one of the most intriguing peculiarities of the moderately anisotropic YBCO is the unusual "butterfly"-shaped angular dependencies of the magnetization,[4] mechanical torque,[5] and critical current density.[6] Of course, it is clear that the phenomenon is strongly linked with the anisotropic nature and distribution of crystal defects, i.e., the anisotropy of quenched disorder, as well as with the anisotropic dynamics of the moved flux-line lattice interacting with the environment. An impressive amount of work has been carried out to elucidate the nature of pinning in HTSC's in general and in YBCO in particular. Nevertheless, the understanding of the main pinning mechanism is still far from complete. In the case of weak point pins, the elementary interaction between an individual flux line and a pinning center is believed to be known and is considered to be calculated with Thuneberg's formalism (see, for example, Ref. 7). Three-dimensional (3D) collective pinning theory provides in this case a reasonable concept for statistical summation of the elementary pinning forces. In this theory only random pointlike quenched disorder is assumed to be effective in HTSC materials.[8] It is quite understandable that oxygen vacancies appear to be acceptable candidates for the random pointlike disorder. However, in YBCO crystals they in fact coexist with at least twin boundaries and dislocations. The extended defects intro-

0163-1829/94/50(18)/13724(11)/$06.00

duce into HTSC's another type of quenched disorder, correlated disorder. The interaction of vortices with a correlated disorder differs significantly[9] but up to date there are no unambiguous experimental results demonstrating it.

In addition there exists an extremely important peculiarity of the flux dynamics in the mixed state called creep, i.e., thermally activated hopping of vortices or their bundles between potential wells under the action of any finite driving force. Creep results in the relaxation of the irreversible states in any nonideal superconductor with pins and, therefore, leads to complications of J_c measurements either by transport-current I-V curves or by magnetization. As a consequence of the supercurrent decay via thermally activated flux creep, the measured value of J_c actually depends upon the electrical field E_c used. This effect appears to be strongly connected with another still unexplained phenomenon, the so-called "fishtail effect" or peak effect. The peak effect is the nonmonotonic dependence of J_c and magnetization upon intermediate values of the applied magnetic fields.[10] After observation of the effect in YBCO SC's,[10,11] its explanation seemed to be closely related to the general understanding of the flux behavior in HTSC's. Later, a similar effect was detected in some MT YBCO samples[12,13] by magnetization measurement; however, it has never been observed in YBCO films to our knowledge. Early explanations of the effect based on the supposed field-induced granularity mediated by oxygen-deficient regions were refuted after experimental evidence of strong coupling in YBCO SC's was obtained.[14] Then it was found that the oxygen content strongly influences the effect.[10,15] Recently, the collective creep theory was attempted to use for the "fishtail" interpretation in the YBCO SC's.[16] The J_c maximum at intermediate field is suggested to arise when the collective-creep-controlled regime with fast flux relaxation is replaced at higher fields by the J_c-(i.e., pinning-) controlled regime with the creep rate substantially slowing down. This model, although interesting as a different approach, in fact does not take into account the remarkable angular dependence of the effect,[6] which might be attributed to the anisotropic nature of the vortex interaction with quenched disorder caused by pointlike (oxygen vacancies) and extended defects (like twin boundaries or/and dislocations).

It should also be noted that a majority of the interpretations of the "fishtail" effect and anisotropic flux dynamics in YBCO SC's are based on results of magnetization experiments, which is a simpler way to define J_c and the pinning parameters in small-sized and brittle samples like YBCO single crystals. The magnetization measurements involve some uncertain factors such as the field-dependent form factor, possible granularity, the influence of the magnetic-moment relaxation rate and external-field ramp rate, etc., thus making an unambiguous interpretation of the experiment not an easy task. Moreover, the magnetization measurements allow one to obtain data on the flux dynamics only in the $J \leq J_c$ regime. In the present work we studied the anisotropy of the flux-line lattice (FLL) dynamics and "fishtail" effect by means of transport-current I-V curve measurements, that is, in the $J \geq J_c$ regime. As a result, the nature of the $J_c(\theta)$ minima and maxima can be understood as well as the fishtail origin and its anisotropy.

II. EXPERIMENT

Having in mind to investigate the FLL behavior connected with the difference sort and degree of quenched disorder, YBCO single crystals and melt-textured YBCO samples were chosen for the study. The single crystals were grown by the standard self-flux method in yttrium-stabilized-zirconia (YSZ) crucibles. The starting charge consisted of a BaO-CuO eutectic mixture with 10 wt % of stoichiometric YBCO. Annealing in a high-pressure oxygen atmosphere yielded a typical single-crystal superconducting transition at 88.5–90 K ($R=0$) with transition width 0.1–0.3 K. The melt-textured YBCO was produced by the float-zone method and had $T_c=91.5$ K ($R=0$) and transition width 0.5 K. The single-grain samples were cut from a solidified YBCO rod and mechanically thinned to 50–30 μm thickness. The sample preparation routine was the same for SC's and MT samples. The sample for transport measurements was a strip 0.1–0.4 mm wide and 2 mm long cleft from the platelet. After surface etching by O_2 plasma, the silver contact pads were vacuum evaporated. 20 μm gold wires bonded by silver epoxy served as current and potential leads. We used the pulse technique for recording the current-voltage characteristics (CVC's). A current pulse with 10 μs duration and 10 A maximal amplitude was transmitted to the sample via a low-impedance (3 Ω) strip line. The line was loaded with sample which is connected in series with a coupling resistance; thus pulse-front smearing through load-line mismatch was eliminated. The amplifying unit consisted of a step-up transformer and wideband low-noise amplifier. The transformer served to match the low impedance of the potential leads and the high input impedance of the amplifier. We paid special attention to reduction of in-phase and out-of-phase interfering voltages and succeeded in damping them below the noise level–0.2 μV in the measurement frequency band. Thus, at an average potential-lead spacing of about 1 mm the electric-field strength reliably detected by the amplifying unit appears to be 10 μV/cm. We adopted the above value as a standard in our J_c definition procedure and in the following, if not specially stated, all J_c values refer to the 10 μV/cm voltage criterion. The external dc magnetic field was generated by an iron-yoke solenoid. The magnetic-field vector was always normal to the transport-current flow direction. The angle θ between the c axis and the field H is assumed to be zero if $H \| c$.

Transport measurements with microsecond pulses are currently not a common lab technique. That is why it is natural to ask whether probing the FLL with such short current pulses will yield data consistent with dc and magnetization results reported by the majority of other groups, where using 10–100 Hz frequency is a usual practice. We refer to an extensive study of the flux-motion regimes in Ref. 17. It was demonstrated that after the external field is ramped to a fixed value with a

sweep rate dB/dt a transient nonlogarithmic flux creep occurs. The duration of the transient stage, that is, the time needed to reach the critical state of the FLL, τ_0, was found to be inversely proportional to the magnetic-field sweep rate dB/dt. Almost the same reasoning is applicable in our case, i.e., there exists a certain transient period after which a balance forms between the pinning and the driving force. We have estimated the self-field ramp rate to be 10^4 T/s, and extrapolating the τ_0 dependence on dB/dt found the transient-stage time to be much shorter than the measurement time window we used. But there exists another limitation on the current pulse width caused by the viscous properties of the FLL. The measurements bandwidth should not exceed the frequency of crossover from pinning-controlled to viscous FLL response. We have made a comparison of pulse and dc CVC's; the difference did not exceed 10% at least at the range of fields and temperatures where dc measurements were possible. We checked the reproducibility of our results on two MT samples (one presented in the paper labeled sample 1) and four SC samples, labeled samples 2, 3, 4, and 5. Crystals 3, 4, and 5 were cleft parallel to the ab plane and to the a,b axis (we made the a and b axes identical through twinning), and the single-crystalline specimen 3 was cleft at 30° to the a,b axis, so that the Lorentz force vector acting upon a vortex was almost parallel to the [110] or [1$\bar{1}$0] direction.

III. RESULTS AND DISCUSSION

A. Static analysis

Figures 1 and 2 compare sets of angular J_c dependencies for the MT sample 1 and sample 2. It is natural to ascribe to the obvious difference between the $J_c(\theta)$ curves

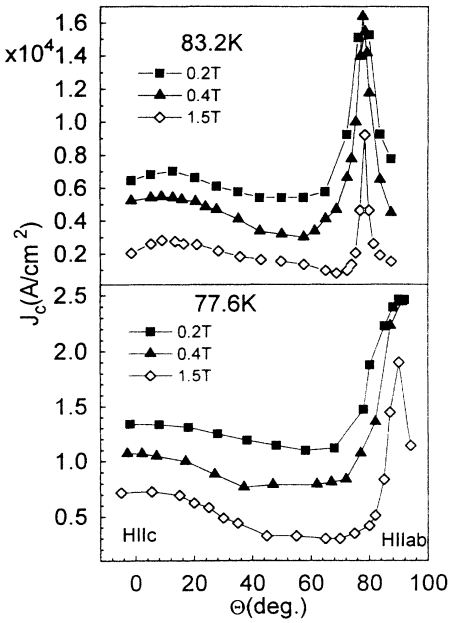

FIG. 1. Angular dependence of J_c for MT sample 1 at various fields and temperatures.

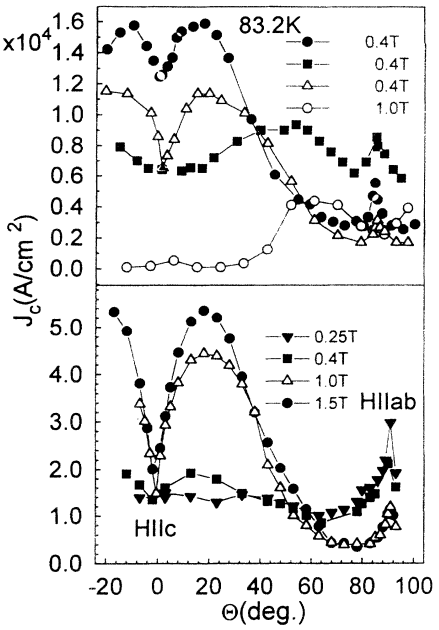

FIG. 2. Angular dependence of J_c for SC sample 2 at various fields and temperatures: 77.6 K (bottom) and for samples 2 (△ and ○), 3 (■), and 4 (●) at various fields (top).

for the two types of samples to different pinning mechanisms in the two cases, resulting in a change of the pinning strength, and first of all to the character of the FLL disorder. Before proceeding to the analysis of the FLL dynamics, we make some preliminary assumptions, based on "static" consideration of the data, and outline in general the microscopic structural features of the two sorts of samples revealed by our x-ray diffraction (XRD), transmission electron microscope (TEM), and high-resolution electron microscopy (HREM) studies. Such a great difference in the anisotropy of J_c as it is easy to see in Figs. 1 and 2 is more or less understandable, since, despite the similarities in structural features inherited from a similar growth mechanism,[13,18] these SC's and single-grain MT samples are characterized by some important distinctions. First of all, our TEM study revealed that widely spaced (0.2–0.5 μm) twin-domain boundaries are the easily observed structural defects in the SC's. We scrutinized the twin-boundary microstructure on the atomic scale by HREM and found no dislocations associated with twins. In contrast, in the MT samples, besides heavy tweedlike twinning, very small inclusions of the 211 phase were noticed as well as dislocation loops usually associated with the 211-123 phase boundary.[13]

Our structural study revealed as well that in both types of samples, as a rule, the polygonal-spiral-mediated mechanism of growth dominates, when the crystals grown are thick enough ($d > 10$ μm). The thicker the crystals, the higher is the density of polygonal spirals and dislocation arrays in the low-angle domain (not be confused with twin domains) sub-boundaries. Slightly in-plane rotationally misoriented (within $\sim 1°$) plateletlike domains appear to be separated from each other by dislocation "walls" detectable with TEM. The average densi-

ty of such edge dislocations involving also some screw components could be estimated as 10^8–10^9 cm^{-2}, and was higher for the MT samples by approximately an order of magnitude. The cores of these dislocations are stretched along the c direction of the crystals within the out-of-plane domain sub-boundaries. They seem to originate from the in-plane rotational misalignment of adjacent platelets. The aspect ratio of the platelets seems to be up to ~ 100. The corresponding in-plane domain sub-boundaries probably consist of arrays of dislocations containing both edge and screw components. The density of these dislocation segments parallel to the *ab* plane is difficult to estimate but it is very important to underline that their length has to scale with respect to the length of the out-of-plane segments like the aspect ratio of the platelike domains. Our structural data will be published elsewhere in more detail.

We obtained no data upon oxygen-vacancy ordering and related effects and derive the integral oxygen content from the well-known linear dependence of the c-axis spacing on δ. For SC samples δ was typically 0.1 ± 0.03, and for MT samples $\delta=0.07\pm0.02$. The SC's appeared to be slightly more oxygen deficient, due to slower oxidation kinetics.

The following argument proposed in Ref. 2 is not unreasonable to relate the shallow bump of the $J_c(\theta)$ curve for the MT sample in the vicinity of the $H\|c$ configuration to dislocation-mediated pinning. The simple model suggested in Ref. 2 neglects collective effects and assumes the bulk pinning force to be proportional to the projection of the intervortex spacing on the *ab* plane, i.e., F_p increases as more vortex lines intersect the cores of the dislocation loops confined to the *ab* planes. This approach leads to the conclusion that in the low-field regime the critical current should depend as $\sim H^{-1/2}$ upon the external magnetic field H (see also below) and the low-angle part of $J_c(\theta)$ should vary as $\sim|\cos(\theta)|^{1/2}$. Indeed, as Fig. 3 demonstrates, the $J_c(H)$ dependencies obey the $\sim H^{-q}$ law fairly well, having a q exponent equal to 0.5 ± 0.05. It is interesting to note that the above-mentioned J_c maximum at $\theta=0$ occurs when $J_c(H)$ deviates from a power function at high fields.

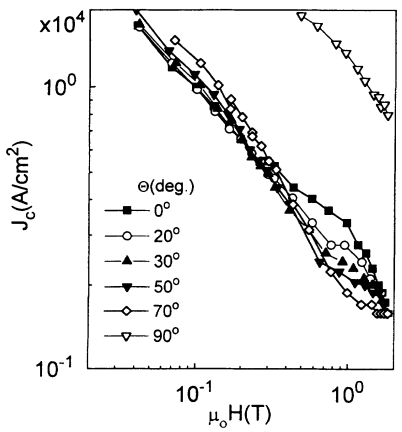

FIG. 3. J_c versus external field for MT sample 1. $T=83.2$ K.

When the external-field direction approaches the c axis, the vortex lines are expected to be liable to fragmentation, forming a steplike pattern. The vortex segments directed along the c axis have to be pinned and trapped by c-axis-extended defects, such as twin planes and dislocation lines.

In the case of high angles, i.e., when the field direction becomes very close to the *ab* plane, it is possible to assume, following Ref. 3, that the vortex segments lying in the *ab* plane are strongly pinned by the intrinsic mechanism or, alternatively, by in-plane extended defects. The intrinsic pinning situation was analyzed in Ref. 3, and the authors obtained a $\sim|\cos(\theta)|^{-1/2}$ dependence for $J_c(\theta)$ in the case of noninteracting vortex fragments, which is probably a real assumption at low fields. Combining the models of Refs. 2 and 3 it seems to be plausible to build up the following picture of the static vortex-pin interaction in the MT samples.

(i) For $\theta<60°$, the vortices may be present as continuous straight lines, interacting with the cores of dislocation loops as point defects; $J_c\sim|\cos(\theta)|^{1/2}$.

(ii) For $88°>\theta>60°$, the vortices are fragmented; the critical current is controlled by c-axis-oriented fragments and $J_c\sim|\cos(\theta)|^{-\alpha}$. This region may be identified by the linear part of the $\log_{10}(J_c)$-$\log_{10}[|\cos(\theta)|]$ plot. As is seen from Fig. 4, the exponent α, defined as the slope of the curve, is 0.65 ± 0.02, in rough agreement with the result of the intrinsic pinning model.[3]

(iii) For $|90-\theta|\leq2°$, the vortices are locked in by the CuO_2 interlayer area and/or by *ab*-plane-confined defects, causing an abrupt upturn in the $J_c(\theta)$ curve.

The most salient feature of the $J_c(\theta)$ curve of single crystals, as Fig. 2 shows, is a sharp drop of J_c at the exact orientation $H\|c$, which evolves into a more gradual decrease as field or temperature increases and the related J_c maximum shifts to higher angles. We also note that the intrinsic peak in the SC's is less pronounced, as compared to that usually encountered in the MT samples. This is very surprising if the intrinsic pinning concept is true because the SC's are much less disordered. Figure 4 shows

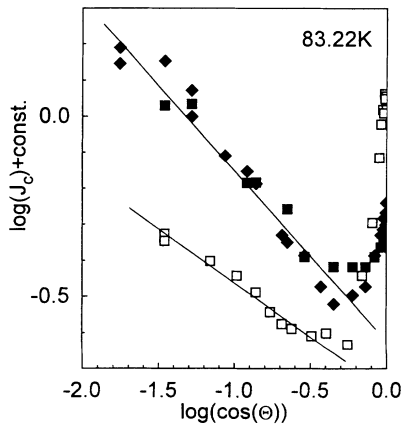

FIG. 4. $\log_{10}(J_c)$ plotted versus $\log_{10}[|\cos(\theta)|]$. The abscissa range corresponds to the 89°–80° interval. Solid lines show $\sim|\cos(\theta)|^{-\alpha}$ approximations. ■, MT sample 1, 0.2 T; ♦, MT sample 1, 0.4 T; □ SC sample 4, 0.4 T.

high-angle $\log_{10}(J_c)$-$\log_{10}[|\cos(\theta)|]$ plots for the single crystal 4; the corresponding α exponent is less than that for MT samples and equal to 0.3 ± 0.02. This obviously may indicate that the "intrinsic" peak is not a generic property of the YBCO material itself but depends to a great extent upon the defect structure of the given specimen.

To reveal the origin of the J_c minimum in the vicinity of the $H\|c$ configuration we plotted $J_c(H)$ curves for various angles between the field and the c axis (Fig. 5) and found that the minimum is linked strongly with the above-mentioned "fishtail" effect. The latter appears to be more pronounced in tilted magnetic fields and partially suppressed at the orientation $H\|c$, which should be a consequence of a superimposed correlated disorder (see below). In Fig. 6 the $J_c(H)$ curves at various angles θ are plotted versus $H\cos(\theta)$; notice that the positions of J_c minima (and maxima) coincide, indicating the major role of the magnetic-field component parallel to the c axis. The field dependencies of the critical current for various temperatures and fixed angle $\theta=50°$ are presented in Fig. 7. Figure 7 shows the temperature dependence of the J_c peak position, and also the temperature-independent slope of the low-field part of $J_c(H)$ when plotted on double-log axes. The corresponding exponent $q=0.58\pm0.6$. Thus we may suppose that $J_c(H)$ in this case is proportional to H^{-q} where q is very close to the value 0.5. The data resemble those reported previously[19] for $2H$-$NbSe_2$ single crystals. Although YBCO single crystals differ in many ways from this low-temperature superconductor, the peak effect, detected for the moderately anisotropic $2H$-$NbSe_2$, probably has a similar origin. In fact, a highlight of Ref. 19 is the convincing experimental verification of 2D collective pinning (2DCP) at low field where the bulk pinning force F_p is proportional to $H^{1/2}$. The onset of the peak is triggered by the transition to a highly disordered three-dimensional FLL and to 3D collective pinning (3DCP) at the field $H_{c0}\approx0.8H_{c2}$. The concept of a dimensional crossover is believed to be still applicable for YBCO, but the fields should be scaled with H_m, i.e., the FLL melting field at a given temperature, while for conventional superconductors H_{c2} is the correct field scale.

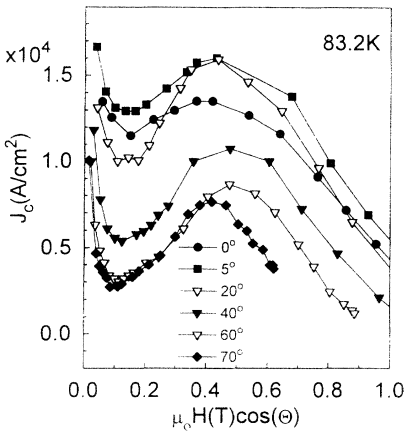

FIG. 6. J_c data from Fig. 4 for SC sample 4 plotted versus $H\cos(\theta)$.

On the other hand, we should assume unambiguously that the 3DCP regime does exist in YBCO. Indeed, it is shown that the correlation length of the vortex lines along the field direction, L_c, is of order of 45 nm.[20] The estimation was done experimentally for the multilayer structure YBCO/PBCO (PBCO is $PrBa_2Cu_3O_7$) and it implies that in a sample with a thickness much larger than 45 nm the 3DCP regime should be valid. In the 3DCP regime[8] $J_c=(W/V_c)^{1/2}H^{-1}$. Here $W\propto H$ is the mean square value of the random pinning force, and $V_c=R_c^2L_c$ is the elastically independent Larkin-Ovchinnikov correlation volume, where $R_c\cong C_{44}^{1/2}C_{66}^{3/2}\xi^2/W$ and $L_c\cong R_c(C_{44}/C_{66})^{1/2}$ are the transverse and longitudinal correlation lengths, respectively. It is easy to see that if L_c does not change and R_c is proportional to $a_0\propto(\Phi_0/B)^{1/2}$, one could suggest single-vortex pinning in this case and, therefore, the collective effects would appear negligible. However, this

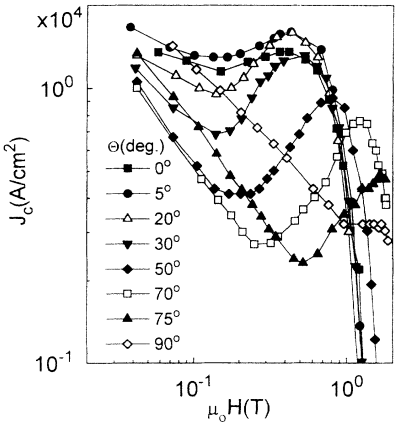

FIG. 5. J_c versus external field for SC sample 4. $T=83.2$ K.

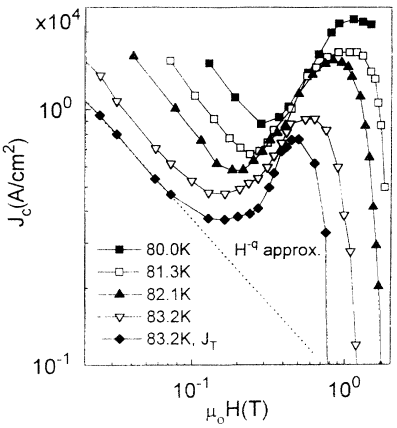

FIG. 7. $J_c(H)$ plots for SC sample 4 at various temperatures; $\theta=50°$. The $J_T(H)$ curve for temperature 83.2 K is also shown along with the low-field H^{-q} approximation (dotted line).

would mean again that we are not taking into account the FLL disorder in the field direction, i.e., we are attempting to force through the concept of the 2DCP regime. If it is really single-vortex pinning with $L_c \leq a_0$,[16] J_c has to be external-field-independent according to the theory of Ref. 8, which was confirmed by some experiments (see, for example, Refs. 16 and 21).

We suggest the most realistic possibility to elucidate the picture is to assume an intrinsic reason for a dimensional crossover. The intrinsic property might be a strong geometrical dispersion for the elastic moduli versus the FL displacement wave vector $\mathbf{k}_\perp=(k_x,k_y)$, i.e., in this case the dimensional crossover would imply the transition from short tilt wavelengths with large $k_\perp$ to longer ones. As was shown in Ref. 22 the condition for constant (nondispersive) elastic moduli of the FLL is not $k_\perp \ll k_{BZ}$ (where $k_{BZ}\approx\pi/a_0$), but rather $k_\perp \ll \lambda^{-1}$. This means the FLL elasticity is nonlocal at distances $<\lambda$ and the tilt modulus $C_{44}(\mathbf{k})$ is highly dispersive if $k\lambda>1$:

$$C_{44}(\mathbf{k})=(B^2/\mu_0)/(1+\lambda_c^2 k_\perp^2+\lambda_{ab}^2 k_z^2)+(B/\Phi_0)P(k_z)\ . \tag{1}$$

Here the first term originates from vortex-vortex interaction and $P(k_z)$ is the line tension of a nearly isolated flux line. At large $k_\perp \gg \lambda_c^{-1}$ (short tilt wavelengths) the tilt energy is dominated by the line tension term, i.e., the FL's behave as if they were isolated.[22] At small $k_\perp \ll \lambda_c^{-1}$ local (nondispersive) elasticity occurs, with $C_{11}\approx C_{44}\approx B^2/\mu_0$. Hence macroscopically uniform deformations are not softened. From this point of view we assume that, while the transverse correlation length R_c remains less than the magnetic penetration depth λ_c along the c direction, the size of the correlation volume V_c is reduced, effectively promoting the isolated vortex regime. Due to softening of the C_{44} tilt modulus the vortices become, not straight lines, but a set of segments, adjusting to random point defects (oxygen vacancies). Thus, in the framework of this assumption, the crossover occurs when the external magnetic field becomes higher and achieves some "critical" level (H_A). This field is in fact the field where collective effects "switch on" and vortex segments start to interact. The collective effects increase J_c versus H abruptly, as shown in Fig. 7. This is a static-picture-based reason for the peak effect.

From this point of view the angular dependence of J_c can be easily understood: if the magnetic field is directed along the c axis the flux lines are trapped by extended defects, twin planes being the most probable structural imperfections of this kind (though the c-oriented dislocation arrays may contribute as well to the correlated disorder and vortex lock-in, it is difficult to estimate their real contribution; therefore in the following discussion we will consider only twins as effective c-oriented extended defects). Thus, the effective tilt modulus is substantially enhanced and its softening is inhibited.

A static analysis of the lock-in transition was undertaken theoretically in Ref. 23. Analyzing the competition between line tension and pinning energy the dependence of the locked segment length upon θ was derived and the unlocking critical angle found to be 14°. If the magnetic-field vector and the Lorentz force vector lie almost within the twin plane, the locking angle is expected to increase. Indeed, the $J_c(\theta)$ curve for single-crystal sample 3 (Fig. 2), prepared as described above (a strip for the CVC measurement was cleft at $\sim 30°$ to the a,b axis), reveals the $H\|c$ minimum to be extended over 60° and the intermediate J_c maximum to be damped. It follows that the widely spaced twin planes are not such effective pinning sites as the much weaker but more numerous point pins—oxygen vacancies (as we will see below the strength of the pinning sites depends strongly upon the dissipation level, i.e., E_c, which is used to define J_c). The locking property of the twins increases the C_{44} modulus of the FLL, but the C_{66} shear modulus remains too soft to prevent flux-line slipping between the twins[9] and along them,[24] while the 2D FL states induced by twins hamper the oxygen vacancies from participating in the pinning process.

The problem of the FLL-twin interaction proves to be a complex one. Our detailed study of it will be published elsewhere; here we mention only the anisotropic character of the twin-plane pinning, i.e., it depends strongly upon the Lorentz force (not only the magnetic-field) orientation with respect to the twin boundary.

Beyond this point a pure static approach seems not to be informative any more and one should combine it with some assumptions about the FLL dynamics, to explore the problem in a more productive manner. The following dynamical study first of all deals with the shape of current-voltage characteristics, as the most reliable source of information on the laws which govern the FLL motion. In the present work we consider two alternative approaches: (a) the thermally-activated-hopping-based models of collective creep,[25] the vortex glass[26] and Bose glass;[9] (b) the classical mean-field model.[27] We test the consistency of each model by fitting the CVC's with model function forms and express the goodness of the fit as a normalized deviation (ND), i.e., the usual mean square root deviation as a percentage of the full Y-coordinate range. The fit is assumed to be consistent if the ND $<1\%$. We will dwell in particular upon the cases where the fit breaks down.

B. Dynamic analysis

1. *Vortex glass, Bose glass, collective creep models*

In the framework of the vortex glass (VG), Bose glass (BG), and collective creep (CC) models the quasiexponential I-V dependence is assumed to arise from thermally activated motion of the vortex ensemble. The resulting current-voltage characteristic is described by the function

$$\frac{E}{J}=\rho_0 \exp\left[-\left[\frac{J_0}{J}\right]^\mu\right]\ . \tag{2}$$

For brevity we will call this function the VG fit. Here the fitting process means a variation of μ till the CVC being replotted in a $\log_{10}(V/I)-1/I^\mu$ scale conforms to a straight line. The $\mu(H)$ curves along with $J_c(H)$ plots for

MT and SC samples are shown in Fig. 8, and $\mu(\theta)$ dependencies are depicted in Fig. 9. For the MT sample the $\mu(H)$ curve resembles strongly the one reported earlier for epitaxial film samples.[28] Following the method proposed in Ref 28, we plotted μ versus current J_c. Our results show that the $\mu(J_c)$ values taken at various fields and temperatures do collapse into a steplike function, and the crossover current at which μ falls from ~ 1 to 0.2 is 2×10^3 A/cm^2. But the scaling fails if the external field is inclined to the c axis at an angle greater than 60°. In the high-angle region the VG fit is still valid, but J_c grows rapidly when H approaches the $H\|ab$ configuration and the μ exponent exhibits a slight maximum, exceeding the average value by 20%. We consider this as a result of the onset of the vortex fragmentation and alternative vortex motion regime.

The VG fits in the case of the SC's give insight into the fishtail-effect problem. First of all, we note for Fig. 9 that for the $H\|c$ and $H\|ab$ configurations $\mu=1.1\pm0.2$, and slightly depends on the magnetic-field magnitude, probably due to interference from the transport-current self-field (~ 10 nT). In the $H\|c$ configuration the vortex lines are locked in by twins, and therefore the situation suits the BG scenario. The BG model expects the μ exponent to be equal to unity, in agreement with our results. The BG state assumes[9] a specific response to a slightly tilted field because the correlated disorder predicts temperature-dependent critical-angle behavior $\theta_c \propto (T_{BG}-T)^{\nu'}$ when $T\to T_{BG}$. Here ν' is the Bose-glass anisotropic correlation length. Indeed, the observation of the μ-exponent behavior in the vicinity of the $H\|c$ configuration allows one to estimate the critical angle θ_c. For the SC sample cleft parallel to the basal axis, i.e., when the transport current flows at 45° to the twin planes and the external-field rotation plane is tilted to the twins with the same angle, the lock occurs with θ within $\sim 2°$ of the $H\|c$ configuration (SC sample 4 in Fig. 9), while for SC sample 3 the corresponding BG locking angle is 10°. (We call the θ interval within which μ does not exceed 1.2 the BG locking angle.) We suppose empirically that

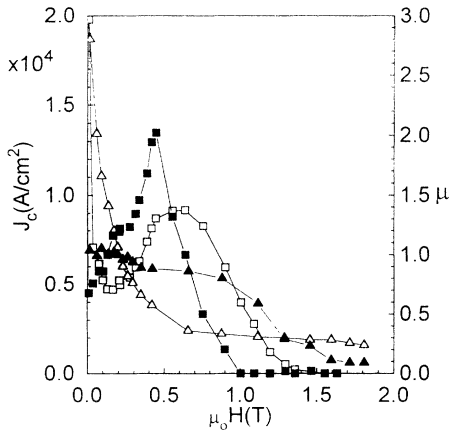

FIG. 8. μ and J_c field dependencies for MT and SC samples; $\theta=50°$, $T=83.2$ K. □, J_c for SC sample 4; △, J_c, for MT sample 1; ■, μ for SC sample 4; ▲, μ for MT sample 1.

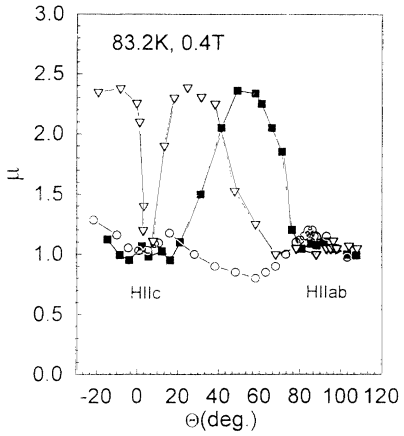

FIG. 9. Comparison of μ angular dependencies for MT and SC samples. The dotted line indicates $\mu=1$ value. ■, SC sample 3; ▽, SC sample 4; ○, MT sample 1.

this angle should be the same as the critical one. This angle is small and should not be confused with the large "static lock-in angle" we dealt with in Sec. III A, i.e., the offset angle at which a length of the vortex segment, captured by the twin, vanishes.

With the c-axis–field angle increasing, the critical current goes up and reaches a maximum at 20°. The J_c increase is accompanied by elevated μ values as Figs. 8 and 9 show. In terms of the glass-based theories we interpret the FLL behavior in this case as a transition from correlated disorder, or a BG state, to a random pointlike disorder, controlled by the FLL–point-defect interaction. The transition occurs over the angle range where the length of the vortex segment locked by the twin boundary is decreasing, and the J_c maximum is attained when the vortex line experiences the twin plane (or dislocation line) as a point defect.

Now we have to discuss the J_c angular and field dependencies in view of the above arguments.

a. $H\|c$. There is pinning by the widely spaced twin planes, i.e., by correlated disorder due to the elastic interaction between pinned and unpinned vortices. The flux dynamics is satisfactory described by the BG model, $\mu\sim 1$. The "fishtail" effect is noticeably suppressed at the $H\|c$ configuration, but nevertheless is quite observable and is accompanied by a slight μ elevation. The critical current falls off as a function $\sim H^{-q}$ of the external magnetic field.

b. Low field and high angles. An example is Fig. 8, $\theta=50°$. The larger angle θ becomes, the closer the $J_c(H)$ plots come to an H^{-q} dependence. The q exponent approaches the value 0.5. This looks like a consequence of the reduction of the superimposed correlated disorder effect (see also Fig. 5). The μ exponent increases with the magnetic field, but still remains less than unity.

c. High fields and high angles. J_c is increasing along with the μ exponent and the VG fit becomes less good; the typical ND is 4–5%; the poorer fit is due to the fitting parameters which become too current dependent.

As the field goes up, J_c comes over a maximum and the μ exponent changes sign—the negative μ values are plotted as zeros in Fig. 8. The change of the μ-exponent sign is often associated with the onset of Kim-Anderson creep, but our analysis of the real CVC form proved, that in this case the CVC's are powerlike and the VG fit is invalid. These results seem sufficient to conclude that the VG model with some amendments, proposed in Ref. 26, is applicable in the case of the more strongly disordered MT samples, for special orientation in the case of SC's, and fails for the comparatively "clean" defect-free SC's (here by "defects" we mean structural defects other than pointlike ones).

We argue that in the case of the FLL interacting with a pointlike quenched disorder, creep-based theories are hardly applicable to the description of the flux dynamics, because thermally activated hopping of the vortices or bundles is not an adequate concept for the moving FLL in the high-velocity regime. Here "high velocity" implies rates of dissipation typical in transport measurements, corresponding to electric-field values, of 0.1–1000 μV/cm, as compared to "low velocity" in the routine flux-relaxation experiments, where E usually is limited to 10^{-1}–10^{-10} μV/cm. In our study we are concerned only with the "high-velocity" regime, the lowest measurable flux velocity being limited by the voltage noise 0.1 μV. Thus we suppose there should exist a region defined by the level of dissipation, between creep-controlled FLL motion and Bardeen-Stephen flow. In this region a key role is played not only by the depth of the pinning well, but also by the form of the pinning potential, the elastic and viscous properties of the FLL. In the forthcoming subsection we discuss implications of the classical approach to the FLL dynamics problem.

2. *Mean-field approximation*

The dynamics of an elastically deformable continuum under the action of a driving force F_{dr} and a random pinning potential was analyzed in Ref. 27. An analytical solution was found for the mean-field approximation (MFA). It was demonstrated in Ref. 27 that in the case of strong pinning there is a nonzero threshold F_T for the driving force F_{dr}; and if $F_{dr} < F_T$ the solution is stable; if $F_{dr} > F_T$ the continuum is moving and its velocity is related to the driving force via the scaling law

$$V = V^+ \left[\frac{I - I_T}{I_T} \right]^{\zeta}, \tag{3}$$

where obvious substitutions were made: velocity $v \rightarrow$ voltage V, force $F \rightarrow$ current I.

Similar scaling was found to describe the CVC's of some low-temperature superconductors[29] and the generation of charge-density-wave harmonics.[30] The threshold current I_T here means the "real" critical current as it would be in the absence of thermal activation. The fitting procedure is reduced to a search for the I_T value which approximates the CVC to a straight line in $\log_{10}(V)$-$\log_{10}(I - I_T)$ coordinates with a minimum of the ND. In the first step of the program J_T is assumed to be equal to J_c. According to the theory V^+ at a given orientation and temperature is a field-independent constant; thus the CVC's being replotted as $\log L_{10}(V)$-$\log_{10}[(I - I_T)/I_T]$ functions should converge in a single line. We found that the Eq. (3) scaling law holds true for the low-field region over the full range of the measurable voltages, but surely we do not exclude effects of thermal activation at low dissipation rates and, as a consequence, of a breakdown of the scaling law. We are aware that the validity of the simplified mean-field approximation for real FLL dynamics analysis is a questionable matter, and we consider Eq. (3) just as an alternative fitting function. But it will be shown below that the scaling property of the fit is a very effective tool for CVC analysis. The field dependences of the fitting parameters J_T and ζ for single-crystal sample 4 are presented in Fig. 10. We assume that there exist three field regions, each of which is characterized by nontrivial changes of the FLL dynamics. The regions are divided by dotted lines in Fig. 10, and the crossover fields are denoted as H_A and H_B.

a. Low fields ($H_{c1} < H < H_A$). J_c decreases as H^{-q} and the CVC's obey the scaling law Eq. (3). The index ζ is universal and equal to 1.5 ± 0.05, close to $\frac{3}{2}$, that is, to an exact MFA result for a shallow slow-changing potential. The goodness of the fit is high, ND $< 1\%$. We observed the predicted CVC scaling, as Fig. 11 illustrates, for fields of 0.05 and 0.1 T. We emphasize an important difference between the low-field behavior of μ and ζ: μ is field and temperature dependent, while ζ is universal within 10% error.

b. Intermediate fields ($H_A < H < H_B$). J_c gradually increases. As we mentioned above, a possible reason for the J_c increase is the dimensional crossover from nonlocal to local behavior of the tilt elastic modulus $C_{44}(\mathbf{k})$, which looks like the transition 2DCP$\rightarrow$3DCP or the transition from the quasi-isolated-vortex-pinning regime to the collectively (i.e., much more strongly) pinned FLL. In this field range the scaling law breaks down and a fit with reasonable accuracy is possible over a restricted range of voltages. The I_T and ζ data presented in Fig. 10

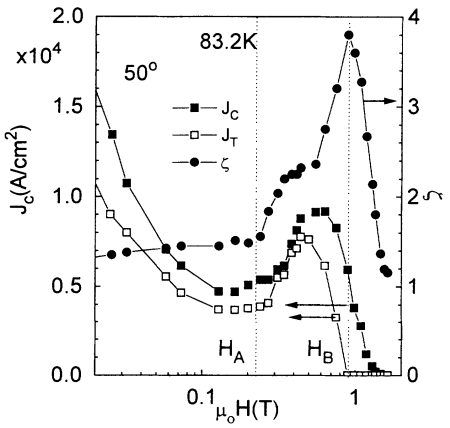

FIG. 10. J_c and MFA fit parameters J_T and ζ as functions of the external fields for SC sample 4. Characteristic field range boundaries are shown by dotted lines.

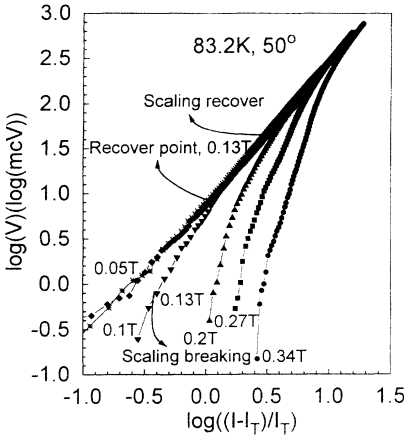

FIG. 11. Current-voltage characteristics for SC sample 4 scaled according to Eq. (3). See explanations in text on J_T parameter usage.

and corresponded to the $H_A < H < H_B$ interval are averaged values, giving a general notion of the parameters' behavior. The situation seems similar to that we encountered when we tried the VG approximation— the fitting parameters are strongly current dependent. But simple reasoning elucidates the origin of the strong I_T dependence. Let us take as proven the fact that the oxygen vacancies are the point defects which cause the FLL disorder and J_c increase and estimate the pinning time t_{pin}, that is, the time the flux line needs to travel over a pinning site; $t_{\text{pin}} = d/v$. Here d is the effective diameter of the pinning site and $v = E/B$ is the velocity of FLL viscous motion. This time is one characteristic time scale and it should be compared with the FLL relaxation time t_{rel}. As a result we obtain a critical flux velocity v_{crit}, at which $t_{\text{rel}} = t_{\text{pin}}$. What does happen if the flux moves so fast that $t_{\text{pin}} \ll t_{\text{rel}}$? The FLL cannot be captured any more by the quickly changing random minima of the pinning potential, and the pinning mechanism caused by the pointlike disorder actually "switches off." For an isolated oxygen vacancy $d \cong 0.3$ nm. Taking typical values $E = 1000$ μV/cm and $B = 1$ T we obtain $t_{\text{pin}} = 10^{-9}$ s. The relaxation time may not be derived so easily, because effects of the vortex entanglement possibly contribute to it. It is very important to understand that t_{rel} defines a time scale for the elastic response of the FLL to an external impact. Following this argument one easily concludes that at high flux velocities and voltages such as $E > E_{\text{crit}}$ the low-field scaling of the CVC's should be restored, because the FLL experiences only a slow-changing pinning potential, such as that induced by the widely and periodically spaced twins. To define the proper I_T parameter for this field interval the low voltage limit of the fitting range should be increased till the scaling recovers. But one may also obtain I_T by approximating the $J_T(H)$ curve from low fields to high ones by some yet unknown function. The most natural approximation is H^{-q} as shown by the dotted line in Fig. 7. Figure 11 shows the CVC plotted on the $\log_{10}(V)$-$\log_{10}[(I - I_T)/I_T]$ scale. Here for the low-field CVC's (0.05 and 0.1 T) the I_T was calculated by the fitting program, and for those which correspond to the "fishtail" field intervals (0.13–0.34 T) I_T was approximated by the H^{-q} function. The plot illustrates the scaling recovery in the high-voltage limit and the scaling breakdown at low voltages. One more obvious implication may be inferred: the J_c angular and field dependencies should depend upon the voltage criterion, E_c, being used. Indeed, Fig. 12 demonstrates that the intermediate J_c maximum gradually disappears when the criterion is elevated. The same procedure being repeated for the $J_c(\theta)$ data set (Fig. 13) yields the expected result: the $H \| c$ minimum becomes more and more shallow and finally transforms to a cusp at high E_c values. This means that now only the twin planes influence the FLL motion in the field of the pinning potential. As a consequence the minimum transforms to its mirror image: a pronounced maximum, because now the twins are the only pinning sites, and therefore the situation becomes extremely simple: the longer the vortex segments trapped by the twins the higher is the critical current density. Thus, by increasing the voltage criterion we probe the contributions of the different pinning sites, which are distinguished from each other by the type of disorder (random or correlated), the range of its action, etc:

(1) At low voltage, twins plus point defects; (2) at higher E_c, twins only; and finally (3) in the linear part of the CVC we obtain the usual ρ_{flow} and J_c angular dependence with a single maximum at $H \| ab$.

c. High fields ($H > H_B$). Here I_T vanishes and the CVC's become simply powerlike. Probably this fact shows some kind of dynamic transition, where the I_T is serving as an order parameter, characterizing flux-pin interaction, i.e., the degree of disorder. The ζ exponent reaches its maximum at the point of transition. It is intuitively clear that the function $(I - I_T)^{\zeta}$ may be smoothly transformed to the power function I^{ζ} if one allows the ζ exponent to grow infinitely when the I_T suddenly becomes zero. Indeed, at the lower temperatures where the

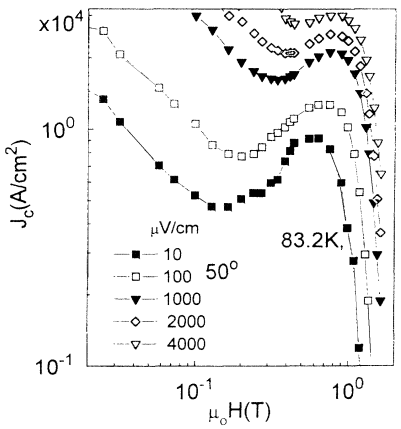

FIG. 12. J_c versus H for SC sample 4. Various electric-field-strength criteria were used.

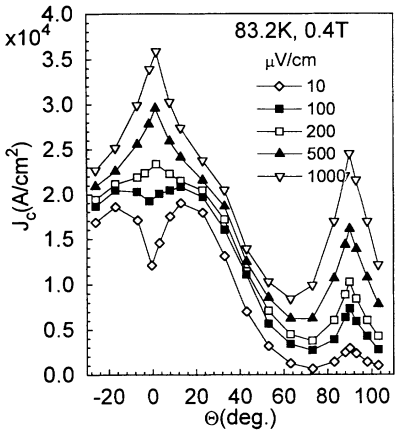

FIG. 13. J_c angular dependencies for SC samples 5 at various electric-field-strength criteria.

$I_T \rightarrow 0$ transition is sharp the ζ-exponent peak value is very high: 20–40. This field interval is absent at $\theta=0$, and I_T vanishes almost simultaneously with J_c, i.e., in the $H \| c$ orientation the twin planes stabilize the vortex lines and the FLL-pin interaction remains strong up to the melting point. We argue that in high fields and at intermediate angles an intermediate phase of the flux forms, on the way from the randomly-point-disordered FLL toward the liquid phase. The main features of the phase are considerably reduced flux-pin interaction and anomalously high viscosity; "dense liquid"[31] seems to be a proper term. Again, we stress the dynamic nature of the phenomena we observe, because, as was shown above, the vortex-pin interaction depends strongly upon the FLL relaxation, and, as a consequence, upon the flux velocity. In the dense-liquid phase the viscosity is high and the relaxation time is estimated as that for a zero-mass oscillator in a viscous medium, e.g., we may obtain $t_{\mathrm{rel}} \simeq \eta/k$, where k is an effective elastic modulus and η is a viscosity. Here we have two competing factors—reduction of the elastic modulus due to the thermal fluctuations and enhanced viscosity due to the vortex entanglement. Thus the viscous liquid may change its properties as $t_{\mathrm{rel}}/t_{\mathrm{pin}}$ changes and turn into the usual vortex glass in the static limit.

IV. CONCLUSION

Let us summarize the main results of the work.

(a) Unusual field and angular dependencies of J_c in YBCO single crystals are a consequence of the flux-lattice transformations: (i) nonlocal, quasi-isolated-vortex behavior of the elastic tilt modulus $C_{44}(\mathbf{k})$ at low field (C_{44} is softened at small defomations); J_c decreasing as a function of field; (ii) crossover to the 3D collective pinning regime at intermediate fields due to the transition to local (nondispersive) behavior of the tilt modulus, "switching on" of the collective effects, and J_c enhancement; (iii) transition to a dense-liquid phase, accompanied by vanishing of the threshold current, J_c goes through a maximum.

(b) The twin planes promote correlated disorder and inhibit the 3D pointlike random disorder as the dominant state for the pinning thus the J_c minimum in the $H \| c$ configuration can be explained.

(c) The "fishtail" effect, being controlled by the vortex interaction with the random point defects, appears to be dynamic in nature and strongly affected by the FLL relaxation process.

(d) The melt-textured samples having a higher degree of disorder due to their real structure exhibit no anomalous behavior and may be envisioned in terms of the usual pinning theory.

We believe the problems which require more studies but have high significance for the matter discussed are as follows:

(a) The suggested role of twin planes should be confirmed by measurements on twin-free single crystals.

(b) There is not enough evidence for oxygen-vacancy pinning as the dominant mechanism in the "fishtail" effect. The hypothesis should be checked by measurements on samples with precise variation of the oxygen content.

(c) The assumed nonlocal-local crossover in the tilt-modulus behavior possibly could be verified by computer simulations.

ACKNOWLEDGMENTS

The authors would like to express gratitude to M. A. Tikhonovski and his colleagues for the MT sample preparation, to V. L. Svetchnikov and H. W. Zandbergen for the thorough TEM and HREM study of the SC's and MT samples, to A. I. Ustinov and V. S. Mel'nikov for the XRD study, and in particular to V. F. Taborov for his invaluable contribution to developing an experimental technique for the pulse I-V curve recording. One of the authors (V.M.P.) is grateful to the DAAD for financial support. Two of the authors (V.F.S. and V.M.P.) greatly appreciate the support of the International Science Foundation. This work has been done partially in the framework of the project "Supercurrent" sponsored by the State Committee of Science & Technology of Ukraine.

[1]B. Roas, L. Schultz, and G. Saemann-Ischenko, Phys. Rev. Lett. **64**, 479 (1990).

[2]V. Selvamanickam, M. Mironova, S. Son, and K. Salama, Physica C **208**, 238 (1993).

[3]M. Tachiki and S. Takahashi, Solid State Commun. **72**, 1083 (1989).

[4]T. I. Arbuzova, I. B. Smoljak, S. V. Naumov, and A. A. Samokhvalov, Supercond. (USSR) **5**, 631 (1992).

[5]Th. Klutsch, R. Hergt, and R. Hiergeist, Physica C **211**, 65 (1993).

[6]V. F. Solovjov, V. M. Pan, and H. C. Freyhardt, in *Proceedings of the 7th IWCC, Alpbach, 1994* [Int. J. Mod. Phys. (to be published)].
[7]E. V. Thuneberg, Cryogenics **29**, 236 (1989).
[8]A. I. Larkin and Yu. N. Ovchinnikov, J. Low Temp. Phys. **34**, 409 (1979); M. V. Feigel'man and V. M. Vinokur, Phys. Rev. B **41**, 8986 (1990).
[9]David R. Nelson and V. M. Vinokur, Phys. Rev. Lett. **68**, 2398 (1992).
[10]M. Daeumling, J. M. Seuntjens, and D. C. Larbalestier, Nature **346**, 332 (1990).
[11]H. Küpfer, I. Apfeldstedt, R. Flükiger, C. Keller, R. Meier-Hirmer, R. Runtsch, A. Turowski, U. Weich, and T. Wolf, Cryogenics **29**, 268 (1989).
[12]H. Küpfer, R. Kresse, R. Meier-Hirmer, K. Salama, D. Lee, and V. Selvamanickam, Physica C **209**, 243 (1993).
[13]M. Ullrich, D. Müller, W. Mexner, M. Steins, K. Heineman, and H. C. Freyhardt, Phys. Rev. B **48**, 7513 (1993).
[14]Y. Ren, P. A. J. deGroot, F. Gencer, and J. S. Abell, Supercond. Sci. Technol. **5**, 49 (1992).
[15]J. L. Vargas and D. C. Larbalestier, Appl. Phys. Lett. **60**, 1741 (1992).
[16]L. Krusin-Elbaum, L. Civale, V. M. Vinokur, and F. Holtzberg, Phys. Rev. Lett. **69**, 2280 (1992).
[17]A. Gurevich and H. Küpfer, Phys. Rev. B **48**, 6477 (1993).
[18]V. M. Pan, V. L. Svetchnikov, V. F. Solovjov, V. F. Taborov, H. W. Zandbergen, and G. Wen, Supercond. Sci. Technol. **5**, 707 (1992).
[19]P. Korevaar, J. Aarts, P. Berhius, and P. H. Kes, Phys. Rev. B **42**, 1004 (1990).
[20]O. Brunner, L. Antognazza, J. M. Triscone, L. Miéville, and Ø. Fisher, Phys. Rev. Lett. **67**, 1354 (1991).
[21]M. Ziese and P. Esquinazi (unpublished).
[22]E. H. Brandt, Phys. Rev. B **48**, 6699 (1993); in *Proceedings of the 7th IWCC, Alpbach, 1994* (Ref. 6).
[23]G. Blatter, J. Rhyner, and V. M. Vinokur, Phys. Rev. B **43**, 7826 (1991).
[24]V. M. Pan, G. G. Kaminsky, A. L. Kasatkin, M. A. Kuznetsov, V. G. Prokhorov, V. L. Svetchnikov, C. G. Tretiatchenko, V. S. Flis, S. K. Yushchenko, V. I. Matsui, and V. S. Mel'nikov, Supercond. Sci. Technol. **4**, S48 (1992).
[25]M. V. Feigel'man, V. B. Geshkenbein, A. I. Larkin, and V. M. Vinokur, Phys. Rev. Lett. **63**, 2303 (1989); M. V. Feigel'man, V. B. Geshkenbein, and V. M. Vinokur, Phys. Rev. B **43**, 6263 (1991).
[26]M. P. A. Fisher, Phys. Rev. Lett. **62**, 1415 (1989).
[27]D. S. Fisher, Phys. Rev. B **31**, 1396 (1985).
[28]C. Dekker, W. Eidelloth, and R. H. Koch, Phys. Rev. Lett. **68**, 3347 (1992).
[29]S. Bhattacharya and M. J. Higgins, Phys. Rev. Lett. **70**, 2617 (1993).
[30]S. Bhattacharya, M. J. Higgins, and J. P. Stokes, Phys. Rev. Lett. **63**, 1503 (1989).
[31]D. R. Nelson and P. Le Doussal, Phys. Rev. B **42**, 10 113 (1990).